THE JOURNAL OF PHYSICAL CHEMISTRY Letters

Letter

pubs.acs.org/JPCL

Molecular Seesaw: How Increased Hydrogen Bonding Can Hinder Excited-State Proton Transfer

Ralph Welsch,[†] Eric Driscoll,[‡] Jahan M. Dawlaty,*[,‡] and Thomas F. Miller, III*[,†]

[†]Division of Chemistry and Chemical Engineering, California Institute of Technology, 1200 East California Blvd., Pasadena, California 91125, United States

[‡]Department of Chemistry, University of Southern California, Los Angeles, California 90089-1062, United States

Supporting Information

ABSTRACT: A previously unexplained effect in the relative rate of excited-state intramolecular proton transfer (ESIPT) in related indole derivatives is investigated using both theory and experiment. Ultrafast spectroscopy [*J. Phys. Chem. A*, **2015**, *119*, 5618−5625] found that although the diol 1,3-bis(2-pyridylimino)-4,7-dihydroxyisoindole exhibits two equivalent intramolecular hydrogen bonds, the ESIPT rate associated with tautomerization of either hydrogen bond is a factor of 2 slower than that of the single intramolecular hydrogen bond in the ethoxy-ol 1,3-bis(2-pyridylimino)-4-ethoxy-7-hydroxyisoindole. Excited-state electronic structure calculations suggest a resolution to this puzzle by revealing a seesaw effect in which the two hydrogen bonds of the diol are both longer than the single hydrogen bond in the ethoxy-ol. Semiclassical rate theory recovers the previously unexplained trends and leads to clear predictions regarding the relative H/D kinetic isotope effect (KIE) for ESIPT in the two systems. The theoretical KIE predictions are tested using ultrafast spectroscopy, confirming the seesaw effect.

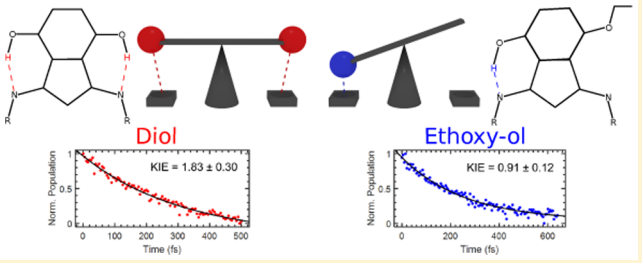

Photocatalytic reactions that couple the electronic and nuclear dynamics are central to many modern chemical challenges, including artificial photosynthesis, carbon dioxide reduction, and nitrogen fixation. Excited-state intramolecular proton transfer (ESIPT)[1−3] is an important example of such reactions that can be studied under controlled conditions using the time-resolved Stokes shift associated with the change in the electronic density during the reaction.

A new class of ESIPT dyes showing a large Stokes shift was recently synthesized[4] and studied both experimentally[4,5] and theoretically.[6,7] This class of ESIPT dyes is particularly interesting as it allows for facile and controllable keto−enol interconversion, leading to potential uses as molecular probes. The ESIPT associated with two particular members of this class (see Figure 1) was studied using ultrafast pump−probe experiments[5] and found to exhibit unusual kinetics. Specifically, the reaction rate for ESIPT in the diol 1,3-bis(2-pyridylimino)-4,7-dihydroxyisoindole was about two times slower than in ethoxy-ol 1,3-bis(2-pyridylimino)-4-ethoxy-7-hydroxyisoindole, despite the fact that there are two protons available for transfer compared to only one proton in ethoxy-ol. The mechanistic basis for this difference was unexplained in previous work.[5]

In this study, we combine excited-state electronic structure calculations, semiclassical transition-state rate theory, and ultrafast pump−probe experiments to explore this effect. First, optimized minimum and transition-state geometries for the lowest singlet excited state are obtained using time-dependent density functional theory (TD-DFT). Then, semiclassical transition-state rate theory (SC-TST) is employed to calculate proton transfer times and predict the relative kinetic isotope effect (KIE) of both molecules. Lastly, the relative KIE of the diol and the ethoxy-ol in acetonitrile is measured using ultrafast pump−probe experiments and compared to the theoretical predictions.

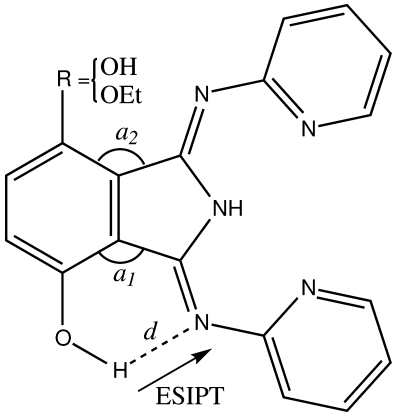

Figure 1. Chemical structures for the diol (R = OH) and the ethoxy-ol (R = OEt). The ESIPT reaction occurs along the indicated hydrogen bond. Geometric parameters are presented in Table 2.

Received: June 23, 2016
Accepted: August 24, 2016
Published: August 24, 2016

ACS Publications © 2016 American Chemical Society

DOI: 10.1021/acs.jpclett.6b01391
J. Phys. Chem. Lett. 2016, 7, 3616−3620

We first demonstrate that intramolecular hydrogen bonds create structural shifts on the lowest singlet excited-state potential energy surface (PES) that favor rapid ESIPT in the ethoxy-ol relative to the diol. Structures, energies, and harmonic vibrational frequencies for the ESIPT reactant and transition state for each molecule on the lowest singlet excited-state surface are obtained using TD-DFT with a range of exchange-correlation functionals and basis sets.[8−14] The current analysis assumes that only a single-proton transfer occurs in the diol, as is consistent with previous studies.[5−7] In particular, the observed similarities for the Stokes shift in the diol and ethoxy-ol suggest that only a single-proton transfer reaction occurs in both systems; additional support for the assumption includes the observation of single-exponential kinetics for ESIPT in both the diol and the ethoxy-ol,[5] as well as calculated barrier heights that indicate the concerted double-proton transfer in the diol to be kinetically unfavorable.[6,7] The harmonic frequencies were calculated for both the protonated and deuterated versions of these molecules, to enable the KIE calculations reported below. The effects of the acetonitrile solvent are included using a polarizable continuum model (PCM)[15,16] (see section IIb in the Supporting Information for full details). Excitation to the singlet excited-state considered in this study is dominated by a HOMO-to-LUMO transition, which exhibits a shift in electronic density from the OH group to the acceptor N;[5] additional analysis of the low-lying excited states is provided in section IIb in the Supporting Information. Figure 2 illustrates optimized geometries for the ESIPT

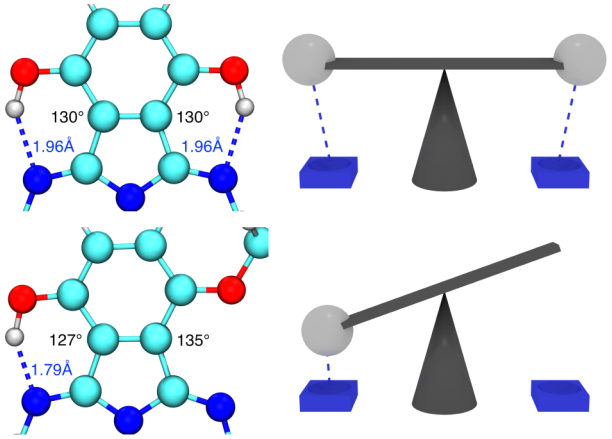

Figure 2. Depiction of the molecular seesaw effect. Optimized geometries for the ESIPT reactant for the diol (top panel) and the ethoxy-ol (bottom panel) are shown from calculations at the B3LYP/TZVP level of theory. ESIPT distances are shown in blue and given in angstroms, and the C−C−C bond angles are shown in black. As illustrated at right, removing one of the hydrogen bonds, as in the ethoxy-ol, eliminates the competition of the two hydrogen bonds and thus shortens the remaining hydrogen bond.

reactant for both molecules. As seen in Figure 2, the balance of the two hydrogen bonds in the diol leads to a symmetric structure. In the ethoxy-ol, however, one of the hydrogen bonds is eliminated and the remaining hydrogen bond is thereby shorter than in the diol. This is reminiscent of a seesaw (Figure 2), in which shortening of the hydrogen bond results in a shorter proton transfer distance and a roughly 20% lower ESIPT barrier height (see Table 1).

We next confirm that the seesaw effect observed in the ESIPT distances is due to the competing attractions of the two

Table 1. Barrier Heights (in Kilocalories per Mole) for ESIPT in the First Excited State of the Diol and the Ethoxy-ol Obtained Using Different Functionals and Basis Sets

method	diol	ethoxy-ol
B3LYP/TZVP	5.4	4.3
B3LYP/6-31++G(d)	5.9	4.8
M062X/6-31++G(d)	5.9	4.7
CAM-B3LYP/6-31++G(d)	5.1	3.7

hydrogen bonds in the diol, rather than steric repulsions in the ethoxy-ol. This is done by first considering an alternative conformation of the ethoxy-ol, in which the R = OEt (i.e., R = OCH_2CH_3) moiety is oriented in a gauche conformation with respect to the iso-indole moiety (see Figure S10), rather than in the anti conformation shown in Figure 2. If steric repulsions are leading to the calculated structural changes in the ethoxy-ol, then this gauche conformation should exhibit an even shorter hydrogen bond. However, comparison of the excited-state minimum geometries of both conformers show very similar hydrogen bond lengths (see Table 2). This finding is

Table 2. Structural Parameters on the First Excited State, S_1, Related to the Seesaw Effect for the Diol, Ethoxy-ol, and Methyl-ol Obtained Using B3LYP/TVZP[a]

R	d	a_1	a_2
OEt-anti	1.79	127°	135°
OEt-gauche	1.74	125°	137°
CH_3	1.77	127°	134°
OH	1.96	130°	130°

[a]For the definition of d, a_1, and a_2, see Fig. 1. Distances given in angstroms.

corroborated by analyzing a third molecule, for which R = Me (i.e., R = CH_3), and it is found that this molecule likewise exhibits a hydrogen-bond length very similar to that of the ethoxy-ol (see Table 2). These results indicate that the geometrical changes shown in Figure 2 are due to the removal of the balance of the two hydrogen bonds in the diol and not due to steric effects in the ethoxy-ol. A similar seesaw effect is found when comparing the ground-state minimum geometries (see section IIf in the Supporting Information).

To investigate if the observed differences in geometry and barrier height account for the experimentally observed difference in ESIPT times, we now present semiclassical rate calculations and experimental rates for the ESIPT in the diol and the ethoxy-ol. For the theoretical work, a separable semiclassical approach is employed and the thermal rate constant $k(T)$ is calculated using[17]

$$k(T) = \kappa\sigma \frac{k_B T}{h} \frac{1}{Q^{r}_{vib,1}} \prod_{i=2}^{F} \frac{Q^{\ddagger}_{vib,i}}{Q^{r}_{vib,i}} e^{-\beta \Delta V} \quad (1)$$

where $\beta = \frac{1}{k_B T}$; σ is the symmetry factor; $Q^{r}_{vib,i}$ denotes the harmonic vibrational partition function of the ith normal mode at the reactant minimum; $Q^{\ddagger}_{vib,i}$ denotes the harmonic vibrational partition function of the ith normal mode at the transition state; and the normal modes are sorted such that the reaction coordinate (i.e., OH stretching mode at the minimum, unstable mode at the transition state) corresponds to $i = 1$. ΔV is the potential energy difference between the reactants and the transition state, and κ denotes a tunneling correction factor

DOI: 10.1021/acs.jpclett.6b01391
J. Phys. Chem. Lett. 2016, 7, 3616−3620

along a separable one-dimensional reaction coordinate (see also section IIa in the Supporting Information):

$$\kappa = \frac{e^{\beta}\Delta E}{1 + e^{2\pi\Delta E/|\omega_I|}} + \frac{1}{2}\int_{-\infty}^{\pi\Delta E/|\omega_I|} d\theta\, e^{\beta|\omega_I|\theta/\pi}\,\mathrm{sech}^2(\theta) \quad (2)$$

where ΔE is the zero-point energy corrected barrier height, defined as $\Delta E = \Delta V + E^{\ddagger}_{ZP} - E^{r}_{ZP}$; $E^{\ddagger}_{ZP}$ and E^{r}_{ZP} are the harmonic zero-point energies at the transition state and the reactant minimum, respectively; $\omega_I = \omega^{\ddagger}_{vib,1}$ is the frequency of the unstable mode at the transition state. Because ESIPT is a first-order process, the reaction transfer time is obtained as $\tau = \frac{\ln(2)}{k(T)}$. TD-DFT calculations are used to obtain the reaction barriers and harmonic vibrational frequencies associated with the excited-state PES (see section IIb in the Supporting Information). Experimentally, the ESIPT transfer times are measured using ultrafast pump−probe experiments in a setup described previously[5] with minor modifications detailed in section I in the Supporting Information. An ultraviolet (UV) pump−visible probe technique was used to measure the femtosecond transient absorption of each compound in acetonitrile. The appearance of a stimulated emission band corresponding to the proton/deuteron transferred photoproduct was fit to a single exponential to extract the ESIPT transfer time and the KIE.

Table 3 presents both the calculated and the measured ESIPT transfer times in the diol and the ethoxy-ol. Comparison

Table 3. Calculated and Measured Proton Transfer Times, τ (in Femtoseconds), of the Diol and the Ethoxy-ol, as Well as the Respective Relative Values

method[a]	molecule	τ	relative
B3LYP/TZVP	diol	2358	1.55
B3LYP/TZVP	ethoxy-ol	1520	
B3LYP	diol	3130	1.44
B3LYP	ethoxy-ol	2177	
M062X	diol	3884	1.41
M062X	ethoxy-ol	2755	
CAM-B3LYP	diol	1259	1.68
CAM-B3LYP	ethoxy-ol	749	
experiment	diol	319 ± 50	1.24 ± 0.24
experiment	ethoxy-ol	257 ± 30	

[a]If not specified, the basis set used is 6-31++G(d).

of the current experimental work (performed in acetonitrile solvent) with previous experimental work[5] (in methanol) reveals that the relative rate for ESIPT in the diol and ethoxy-ol is relatively insensitive to solvent effects. The calculated transfer times are obtained with parameters from TD-DFT calculations employing different exchange-correlation functionals and basis sets. For all functionals and basis sets the calculated transfer times in the ethoxy-ol are significantly shorter than in the diol, which is consistent with the experimentally observed trend and the observation that the ethoxy-ol exhibits a shorter proton transfer distance (see Figure 2). However, the calculated values of the ESIPT transfer time depends strongly on the functional employed, which hinders the direct comparison to experiment. Table 3 also shows that the relative value of the ESIPT transfer times for the diol versus the ethoxy-ol is more robust across the different functionals, yielding reasonable agreement with the experimental value of 1.24 ± 0.24. The robustness of these calculated relative transfer times is due to the fact that the height of the ESIPT barrier predicted by a given functional for the two molecules is strongly correlated (see Figure 3).

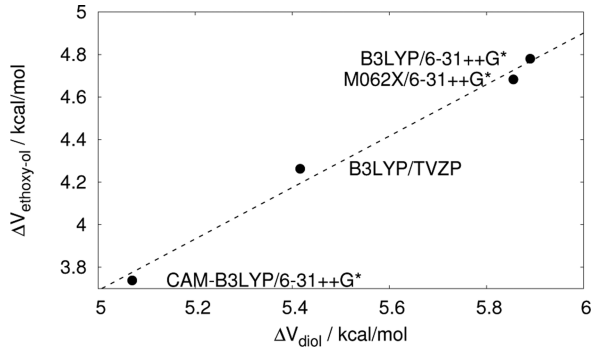

Figure 3. Correlation of barrier heights (in kilocalories per mole) in the diol and the ethoxy-ol when employing different exchange-correlation functionals and basis sets.

Next, the rate calculations are used to predict the relative H/D KIE for the ESIPT reactions. Table 4 and Figure 4 present

Table 4. Calculated and Measured KIE of the Diol and the Ethoxy-ol, as Well as the Respective Relative Values

method[a]	molecule	KIE	relative
B3LYP/TZVP	diol	7.67	1.42
B3LYP/TZVP	ethoxy-ol	5.42	
B3LYP	diol	8.74	1.39
B3LYP	ethoxy-ol	6.28	
M062X	diol	9.05	1.41
M062X	ethoxy-ol	6.41	
CAM-B3LYP	diol	6.88	1.55
CAM-B3LYP	ethoxy-ol	4.44	
experiment	diol	1.83 ± 0.30	2.01 ± 0.42
experiment	ethoxy-ol	0.91 ± 0.12	

[a]If not specified, the basis set used is 6-31++G(d).

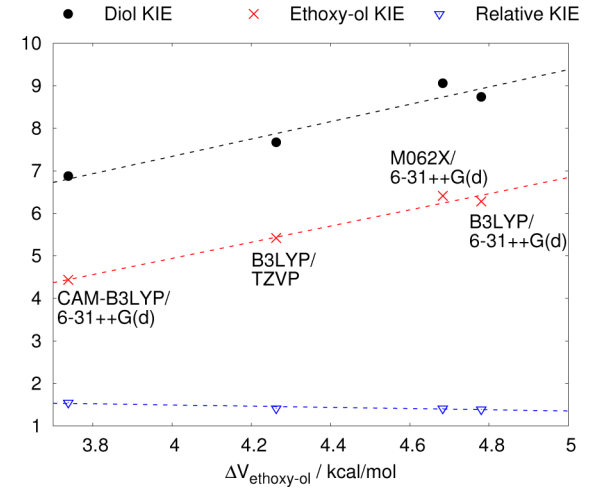

Figure 4. Absolute and relative (i.e., diol/ethoxy-ol) KIEs obtained at various levels of theory as a function of the ESIPT barrier height for the ethoxy-ol. The experimentally measured relative KIE is 2.01 ± 0.42, and the range of values for the calculated relative KIE is 1.39−1.55.

DOI: 10.1021/acs.jpclett.6b01391
J. Phys. Chem. Lett. 2016, 7, 3616−3620

the calculated KIEs, obtained at various levels of theory. Also reported are the calculated relative (diol/ethoxy-ol) KIE values, which are typically greater than one, due to the higher barrier for ESIPT in the diol. As for the calculated transfer times, the absolute values for the KIE calculations are more sensitive to the level of theory than the relative KIE values (which vary by less than 10% across levels of theory). Thus, the relative KIE values are best suited for comparison with experiment.

Table 4 also reports experimentally measured KIE for the two ESIPT reactions. Although the absolute values of the measured KIEs are smaller than the calculated values (which is consistent with the fact that the calculated transfer times for these reactions are typically larger than the corresponding experimental values in Table 3), the calculated relative KIE values in the range of 1.39−1.55 are in reasonably good agreement with the experimentally observed value of 2.01 ± 0.42.

In summary, the counterintuitive experimental observation[5] of faster ESIPT in the ethoxy-ol than in the diol is ascribed to a seesaw effect (Figure 2) in which a reduction in the number of intramolecular hydrogen-bond interfaces leads to a reduction in the ESIPT transfer distance. Using SC-TST calculations with parameters from TD-DFT calculations, it is predicted that this seesaw effect will lead to a larger KIE for the diol than the ethoxy-ol, which is experimentally confirmed using ultrafast spectroscopy. We note that although good agreement is found for the relative transfer times and relative KIE between the two molecules (Tables 3 and 4), the absolute KIEs (Table 4) and transfer times (Table 3) exhibit differences among the levels of theory and between theory and experiment. These issues are due to the approximations associated with the exchange-correlation functionals (Figures 3 and 4), possibly in addition to approximations associated with the use of a TST description for a reaction with a relatively low barrier (see section IId in the Supporting Information). Quantum dynamics methods, e.g., the ring-polymer molecular dynamics approach,[18,19] can be used to investigate possible nonequilibrium effects related to sudden photoexcitation,[20−22] which will be the focus of future work. The similarity of the relative ESIPT transfer times for diol and ethoxy-ol in acetonitrile versus that in methanol[5] suggests that the seesaw effect is relatively robust to the solvent environment, including some protic solvents; nonetheless, we recognize that solvent environments that disrupt the intramolecular hydrogen bonds of the diol and ethoxy-ol would likewise be expected to disrupt the seesaw effect. Finally, although the reported agreement between theory and experiment for the kinetic isotope effects provides additional validation of the assumption of a kinetically limiting single-proton transfer in the diol,[5−7] the dynamics of double-proton transfer in the diol may be of interest for future work.

It is possible that the seesaw effect presented in this work may be exploited in catalyst design with the aim of modulating hydrogen bonding. It is known that minute perturbations in hydrogen bonding can alter the function of redox catalysts that require proton transfer.[23−26] It may be worthwhile to explore design themes in which the strength of hydrogen bonding in the core of a catalyst is finely modulated (and perhaps photochemically actuated) by a counterbalanced hydrogen bond located farther away. To realize such goals, it is necessary to study this effect further. For example, if the fulcrum of the seesaw is composed of a single C−C bond and hydrogen bonds are placed along the body of the seesaw at variable distances, a potential extension of the mechanical "law of the lever" to molecular scales may be achievable.

■ ASSOCIATED CONTENT

Supporting Information

The Supporting Information is available free of charge on the ACS Publications website at DOI: 10.1021/acs.jpclett.6b01391.

Details on the experimental setup and the calculations (PDF)

■ AUTHOR INFORMATION

Corresponding Authors

*E-mail: dawlaty@usc.edu.

*E-mail: tfm@caltech.edu.

Notes

The authors declare no competing financial interest.

■ ACKNOWLEDGMENTS

The authors thank Stuart Althorpe and Feizhi Ding for helpful discussions. T.F.M. acknowledges financial support from the National Science Foundation (NSF) CAREER Award under Grant CHE-1057112 and the U.S. Department of Energy under Grant DE-SC0006598. R.W. acknowledges financial support from the *Deutsche Forschungsgemeinschaft* (WE 5762/1-1). E.D. and J.M.D. acknowledge financial support from the AFOSR YIP Award (FA9550-13-1-0128). This research used resources of the National Energy Research Scientific Computing Center, a DOE Office of Science User Facility supported by the Office of Science of the U.S. Department of Energy under Contract No. DE-AC02-05CH11231.

■ REFERENCES

(1) Formosinho, S. J.; Arnaut, L. G. Excited-State Proton Transfer Reactions II. Intramolecular Reactions. *J. Photochem. Photobiol., A* **1993**, *75*, 21−48.

(2) Douhal, A.; Lahmani, F.; Zewail, A. H. Proton-Transfer Reaction Dynamics. *Chem. Phys.* **1996**, *207*, 477−498.

(3) Agmon, N. Elementary Steps in Excited-State Proton Transfer. *J. Phys. Chem. A* **2005**, *109*, 13−35.

(4) Hanson, K.; Patel, N.; Whited, M. T.; Djurovich, P. I.; Thompson, M. E. Substituted 1,3-Bis(imino)isoindole Diols: A New Class of Proton Transfer Dyes. *Org. Lett.* **2011**, *13*, 1598−1601.

(5) Driscoll, E.; Sorenson, S.; Dawlaty, J. M. Ultrafast Intramolecular Electron and Proton Transfer in Bis(imino)isoindole Derivatives. *J. Phys. Chem. A* **2015**, *119*, 5618−5625.

(6) Su, Y.; Chai, S. A TDDFT Study of the Excited-State Intramolecular Proton Transfer of 1,3-Bis(2-pyridylimino)-4,7-dihydroxyisoindole. *J. Photochem. Photobiol., A* **2014**, *290*, 109−115.

(7) Ma, C.; Yang, Y.; Li, C.; Liu, Y. TD-DFT Study of the Double Excited-state Intramolecular Proton Transfer Mechanism of 1,3-Bis(2-pyridylimino)-4,7-dihydroxyisoindole. *J. Phys. Chem. A* **2015**, *119*, 12686−12692.

(8) Lee, C.; Yang, W.; Parr, R. G. Development of the Colle-Salvetti Correlation-Energy Formula into a Functional of the Electron Density. *Phys. Rev. B: Condens. Matter Mater. Phys.* **1988**, *37*, 785.

(9) Becke, A. D. Density-Functional Thermochemistry. III. The Role of Exact Exchange. *J. Chem. Phys.* **1993**, *98*, 5648−5652.

(10) Yanai, T.; Tew, D. P.; Handy, N. C. A New Hybrid Exchange-Correlation Functional Using the Coulomb-Attenuating Method (CAM-B3LYP). *Chem. Phys. Lett.* **2004**, *393*, 51−57.

(11) Zhao, Y.; Truhlar, D. G. The M06 Suite of Density Functionals for Main Group Thermochemistry, Thermochemical Kinetics, Noncovalent Interactions, Excited States, and Transition Elements: Two New Functionals and Systematic Testing of Four M06-Class

DOI: 10.1021/acs.jpclett.6b01391
J. Phys. Chem. Lett. 2016, 7, 3616−3620

Functionals and 12 Other Functionals. *Theor. Chem. Acc.* **2008**, *120*, 215−241.
(12) Schäfer, A.; Horn, H.; Ahlrichs, R. Fully Optimized Contracted Gaussian Basis Sets for Atoms Li to Kr. *J. Chem. Phys.* **1992**, *97*, 2571−2577.
(13) Schäfer, A.; Huber, C.; Ahlrichs, R. Fully Optimized Contracted Gaussian Basis Sets of Triple Zeta Valence Quality for Atoms Li to Kr. *J. Chem. Phys.* **1994**, *100*, 5829−5835.
(14) Dill, J. D.; Pople, J. A. Self-Consistent Molecular Orbital Methods. XV. Extended Gaussian-type Basis Sets for Lithium, Beryllium, and Boron. *J. Chem. Phys.* **1975**, *62*, 2921−2923.
(15) Improta, R.; Barone, V.; Scalmani, G.; Frisch, M. J. A State-Specific Polarizable Continuum Model Time Dependent Density Functional Theory Method for Excited State Calculations in Solution. *J. Chem. Phys.* **2006**, *125*, 054103.
(16) Improta, R.; Scalmani, G.; Frisch, M. J.; Barone, V. Toward Effective and Reliable Fluorescence Energies in Solution by a New State Specific Polarizable Continuum Model Time Dependent Density Functional Theory Approach. *J. Chem. Phys.* **2007**, *127*, 074504.
(17) Fermann, J. T.; Auerbach, S. Modeling Proton Mobility in Acidic Zeolite Clusters: II. Room Temperature Tunneling Effects from Semiclassical Rate Theory. *J. Chem. Phys.* **2000**, *112*, 6787−6794.
(18) Craig, I. R.; Manolopoulos, D. E. Quantum Statistics and Classical Mechanics: Real Time Correlation Functions from Ring Polymer Molecular Dynamics. *J. Chem. Phys.* **2004**, *121*, 3368.
(19) Habershon, S.; Manolopoulos, D. E.; Markland, T. E.; Miller, T. F. Ring-Polymer Molecular Dynamics: Quantum Effects in Chemical Dynamics from Classical Trajectories in an Extended Phase Space. *Annu. Rev. Phys. Chem.* **2013**, *64*, 387−413.
(20) Chudoba, C.; Lutgen, S.; Jentzsch, T.; Riedle, E.; Woerner, M.; Elsaesser, T. Femtosecond Studies of Vibrationally Hot Molecules Produced by Intramolecular Proton Transfer in the Excited State. *Chem. Phys. Lett.* **1995**, *240*, 35−41.
(21) Chudoba, C.; Riedle, E.; Pfeiffer, M.; Elsaesser, T. Vibrational Coherence in Ultrafast Excited State Proton Transfer. *Chem. Phys. Lett.* **1996**, *263*, 622−628.
(22) Lochbrunner, S.; Wurzer, A. J.; Riedle, E. Microscopic Mechanism of Ultrafast Excited-State Intramolecular Proton Transfer:? A 30-fs Study of 2-(2′-Hydroxyphenyl)benzothiazole. *J. Phys. Chem. A* **2003**, *107*, 10580−10590.
(23) Pollack, R. M. Enzymatic Mechanisms for Catalysis of Enolization: Ketosteroid Isomerase. *Bioorg. Chem.* **2004**, *32*, 341−353. Mechanistic Enzymology.
(24) Huynh, M. H. V.; Meyer, T. J. Proton-Coupled Electron Transfer. *Chem. Rev.* **2007**, *107*, 5004−5064.
(25) Solis, B. H.; Hammes-Schiffer, S. Substituent Effects on Cobalt Diglyoxime Catalysts for Hydrogen Evolution. *J. Am. Chem. Soc.* **2011**, *133*, 19036−19039.
(26) Scottwell, S. O.; Crowley, J. D. Ferrocene-Containing Non-Interlocked Molecular Machines. *Chem. Commun.* **2016**, *52*, 2451−2464.

DOI: 10.1021/acs.jpclett.6b01391
J. Phys. Chem. Lett. 2016, 7, 3616−3620